Biosensors and Bioelectronics 55 (2014) 446–451

Contents lists available at ScienceDirect

Biosensors and Bioelectronics

journal homepage: www.elsevier.com/locate/bios

Electrochemical sensor based on carbon-supported $NiCoO_2$ nanoparticles for selective detection of ascorbic acid

Xin Zhang [a], Sha Yu [b], Wenya He [b], Hiroshi Uyama [c,*,1], Qianjie Xie [b], Lu Zhang [b], Fengchun Yang [b,c,*,2]

[a] Shaanxi Provincial Key Laboratory of Electroanalytical Chemistry, Institute of Analytical Science, Northwest University, Xi'an, Shaanxi 710069, China
[b] Key Laboratory of Synthetic and Natural Functional Molecule Chemistry (Ministry of Education), College of Chemistry and Material Science, Northwest University, Xi'an 710069, China
[c] Department of Applied Chemistry, Graduate School of Engineering, Osaka University, Suita, Osaka 565-0871, Japan

ARTICLE INFO

Article history:
Received 8 October 2013
Received in revised form
20 December 2013
Accepted 20 December 2013
Available online 30 December 2013

Keywords:
Electrochemical sensor
Ascorbic acid
Ni
Co
Dopamine
Uric acid

ABSTRACT

An electrochemical sensor for selective detection of ascorbic acid (AA) in the presence of dopamine (DA) and uric acid (UA) was fabricated by modifying the glassy carbon electrode (GCE) with carbon-supported $NiCoO_2$ ($NiCoO_2$/C) nanoparticles. The electrochemical impedance spectroscopic (EIS) studies reveal the little charge transfer resistance for the modified electrode. The electrocatalytic activity of the modified electrode for the oxidation of AA was investigated. The current sensitivity of AA was enhanced to about five times upon modification. The voltammetric response of AA was well resolved from the responses of DA and UA, and the oxidation potential of AA was negatively shifted to −0.20 V. The biosensor tolerated a wide linear concentration range for AA, from 1.0×10^{-5} M to 2.63×10^{-3} M (R^2=0.9929), with a detection limit of 0.5 μM (S/N=3). Our results demonstrate that the $NiCoO_2$/C nanomaterials has excellent AA sensing capability, including a fast response time, high reproducibility and stability, with great promise in the quantification of AA in real samples. That makes it a unique electrochemical sensor for the detection of AA which is free from the interference of DA, UA and other interferents.

1. Introduction

Ascorbic acid (AA) is widely used as an antioxidant in food, animal feed, beverages, pharmaceutical formulations and so on (Kumar et al., 2008). Because of biological and technological importance of AA, accurate determination of AA is essential to food quality and health care. Various methods have been developed to determine AA content, including titrimetry, fluorimetry, voltammetry, flow injection analyses, spectrophotometry, solid-phase iodine method, and liquid chromatography (Hossu, Magearu, 2004). Among them, electroanalysis is sensitive, simple and inexpensive (Zhang et al. 2013b). However, there exist some challenges to measure AA under physiological conditions. The primary challenges are the very low levels of AA and the interference of coexisting dopamine (DA) and uric acid (UA) in organisms, which sharing a similar oxidation potential in electrochemical detection. Thus, it is desirable for diagnostic applications to develop a simple and rapid method for the determination of AA with high selectivity and sensitivity (Liu et al., 2012). And modification of bare electrodes with nanomaterials as the redox active site has been a major goal of much research (Ragupathy et al., 2010; Wen et al., 2010).

Recently, more and more interest has been focused on cheap transition metal oxides, such as nickel oxide (NiO) and cobalt oxide (CoO), because they have multiple oxidation states for electron-transfer processes (Rafiee, Fakhari, 2013). But the alternatives to improve the activity of a mono-oxide are rather limited. So mixed oxides are of special interest through synergistic effects arising from the intimate electronic interaction of the components (Wu et al., 2004; Bertoncello et al., 1999; Cattarin et al., 2001). One of the most promising materials based on transition metal oxides is the mixed Ni and Co oxide, which is, moreover, a stable and cheap electrode material. It was proved that the addition of cobalt to nickel oxide/hydroxide enhances the electrochemical performance of the electrodes (Armstrong et al., 1988; Yuan and Xu, 2001). On the other hand, Ni doped cobalt oxide also enhanced the overall electrical conductivity of the material (Chang et al., 2012).

There are confirmations in the literature that mixing Ni and Co oxides brings beneficial effects on their electrocatalytic activity, but most of the studies were directed toward the use of electrode materials for supercapacitors (Srinivasan and Weidner 2000; Yoon and Ko 2008; Nam and Kim, 2002; Lin et al.,1998; Cao et al., 2005), and oxygen evolution reactions (King and Tseung 1974; Rashkova et al., 2002; Unates et al., 1992; Gennero de

* Corresponding authors.
E-mail addresses: uyama@chem.eng.osaka-u.ac.jp (H. Uyama), fyang@nwu.edu.cn (F. Yang).
[1] Tel.: +81 6 6879 7364; fax: +81 6 6879 7367.
[2] Tel.:/fax: +86 29 88302604.

0956-5663/$ - see front matter © 2014 Elsevier B.V. All rights reserved.
http://dx.doi.org/10.1016/j.bios.2013.12.046

Chialvo, Chialvo 1993; Serebrennikova and Birss 1997). However, the electrocatalytical behavior of mixed Ni and Co oxides for biologic compounds is yet to be investigated extensively. Recently, the preparation of a CNT-nickel-cobalt oxide modified graphite screen printed electrode and its use in the electrocatalytic oxidation of insulin was reported by Arvinte et al. (2010). Ni and Co oxides exhibit interesting electrocatalytic activities, which make them attractive for analytical applications due to the appropriate compromise between electrocatalytic activity, long-term stability and cost.

To the best of our knowledge, electrochemical biosensors for AA based on Ni and Co oxides have not been reported yet. In the present study, $NiCoO_2$ nanoparticles (NPs) are synthesized by controlled coreduction in oleylamine as a reducing agent and dispersed on carbon black to produce carbon-supported $NiCoO_2$ catalysts ($NiCoO_2$/C). The physicochemical properties and electrochemical activities of the NPs for AA oxidation are investigated. Results indicate that $NiCoO_2$/C modified glassy carbon electrode (GCE) exhibited favorable electron transfer kinetics and electrocatalytic activity towards the oxidation of AA. Complete peak separation between AA and DA/UA was observed at the $NiCoO_2$/C modified GCE, and AA can be detected with good sensitivity and selectivity.

2. Experimental

2.1. Reagents and materials

$Ni(NO_3)_2$, $Co(NO_3)_2$, oleylamine (OAm, technical grade, 70%, Aldrich), oleic acid (OA, technical grade, 90%, Aldrich), carbon black (Kejen EC 300J), acetic acid (ACS reagent, g 99.7%, Aldrich). Nafion (5 wt.%) were purchased from Sigma–Aldrich. AA was from the Chemical Reagent Company of Tianjin (China); DA and UA from Alfa Aesar; 0.1 M KOH and 0.1 M phosphate buffer solution (PBS, pH 7.4) was employed as a supporting electrolyte. Rod GCEs were from the Chenhua Co. Ltd. (Shanghai, China). All other Chemicals and reagents for electrochemical measurements were of analytical grade and used without further purification. The deionized (DI) water for solution preparation was from a Millipore Autopure system (18.2 MΩ, Millipore Ltd., USA).

2.2. Preparation of $NiCoO_2$/C modified GCE

Briefly, $NiCoO_2$ NPs were first prepared by controlled coreduction in oleylamine as a reducing agent and dispersed on carbon black to produce $NiCoO_2$/C catalysts. Then the $NiCoO_2$/C as prepared was modified on GCE by general drop-coating method (for the detailed preparation process see the Supporting information).

2.3. Apparatus

All the electrochemical measurements were carried out using a CHI 660D electrochemical workstation (CH Instruments, Shanghai, China). A conventional three-electrode system, consisting of a modified GCE as the working electrode (working electrode area: 0.071 cm^2), and a saturated Ag/AgCl electrode as a reference electrode, a platinum wire as an auxiliary electrode, was employed. EIS was performed with the same three-electrode configuration in an electrolyte solution of 0.1 M KCl containing 1.0 mM $[Fe(CN)_6]^{4-/3-}$, in a frequency range from 0.1 to 10^5 Hz with an AC probe amplitude of 50 mV.

XRD profiles obtained (XRD-6000, Shimadzu) with high-intensity Cu Kα radiation ($\lambda = 1.5406$ Å). Morphologies of $NiCoO_2$ NPs were determined using scanning electron microscopy (SEM) (JEOL JEM-2100).

3. Results and discussion

3.1. Characterization of $NiCoO_2$/C

The TEM images depicted in Fig. 1A show the direct morphological observations of the as-prepared $NiCoO_2$ NPs. In Fig. 1A, it can be seen that the $NiCoO_2$ NPs are well distributed and relatively homogeneous, with their diameter measured to be around 20 nm. The particle size is much smaller than other literatures reported (Arvinte et al., 2010; Chang et al., 2012), which is important for obtaining the higher electrochemical activity.

To obtain the further crystallographic information of the prepared NPs, an XRD measurement was conducted. The XRD pattern for $NiCoO_2$ (Fig. 1B) catalyst shows well-defined diffraction peaks that are indexed to the (111) (200) (220) and (311) planes of $NiCoO_2$ face-centered cubic (fcc) crystal structure (JCPDS 10-0188). Besides that, the little peak at 78.87° may be ascribed to the (222) plane of cubic NiO system, indicating that the presence of some

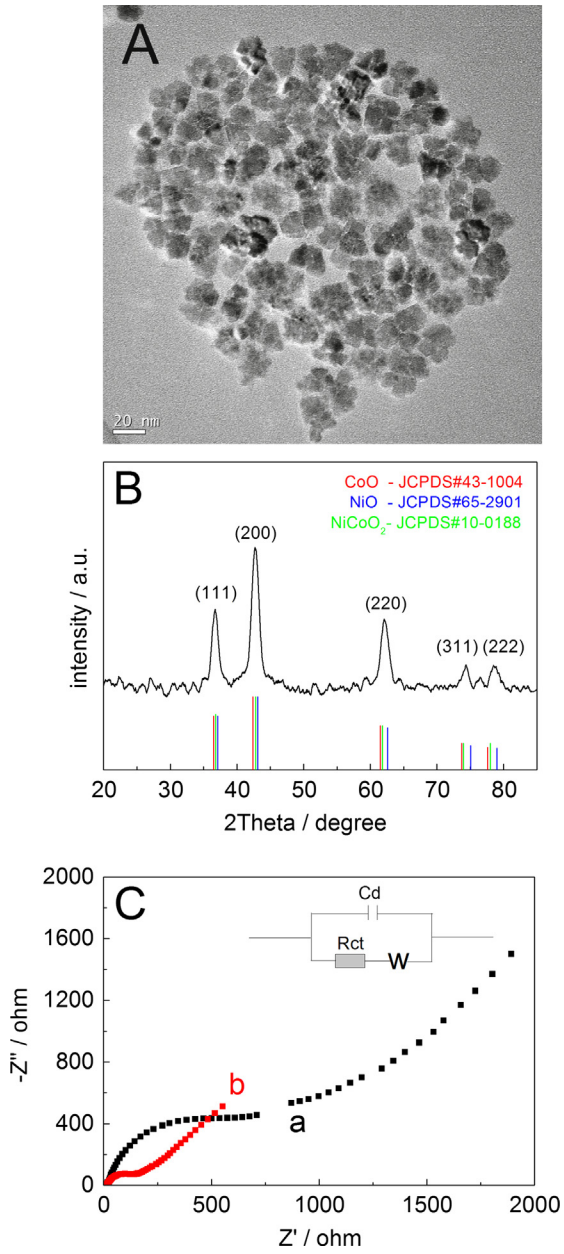

Fig. 1. (A) TEM image and (B) XRD patterns of $NiCoO_2$ nanocrystals. (C) EIS of bare GCE (a) and $NiCoO_2$/C modified GCE (b).

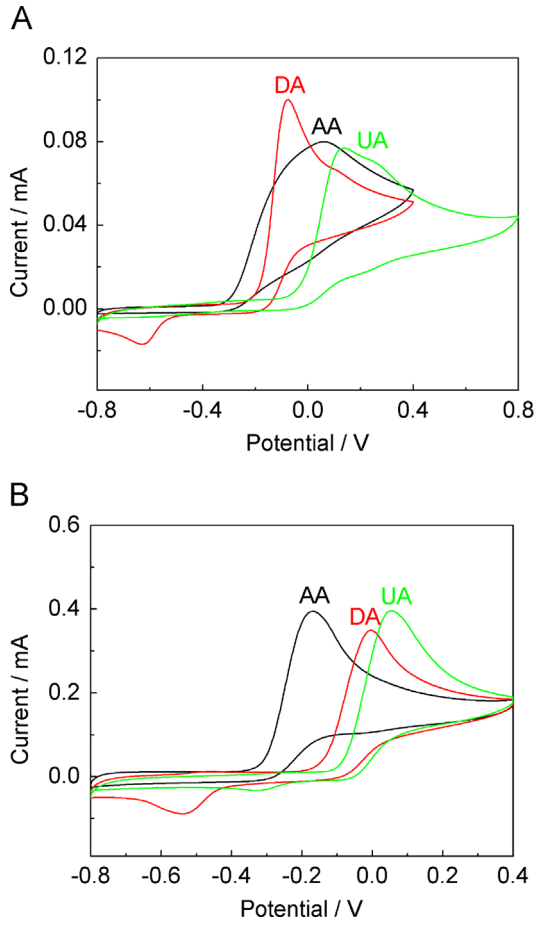

Fig. 2. CVs of 10.0 mM AA, 5.0 mM DA and 10.0 mM UA in 85 mM PBS+5 mM KOH (pH 12.0) at (A) bare GCE and (B) $NiCoO_2$/C modified GCE at a scan rate of 20 mV/s.

more nickel oxide. As revealed in Fig. 1B, no detectable diffraction peaks of metallic Ni or Co were observed in the present study.

Furthermore, EIS is an efficient tool for studying the interface properties of the surface-modified electrodes. The charge-transfer resistance (Rct) at the electrode surface is equal to the semicircle diameter of EIS plot and can be used to describe the interface properties of the electrode. Fig. 1C indicates the results for the impedance spectrum on bare GCE (a) and $NiCoO_2$/C modified GCE (b) in a solution of 1.0 mM $Fe(CN)_6^{3-/4-}$ in 0.1 M KCl. The Randles circuit (inset of Fig. 1C) was chosen to fit the impedance data obtained. It is found that $NiCoO_2$/C modified GCE has a lower charge-transfer resistance value than bare GCE, implying that the introduction of the $NiCoO_2$ plays an important role in providing the conducting bridges for the charge transfer of $Fe(CN)_6^{3-/4-}$.

3.2. AA sensing using cyclic voltammetry

Electrochemical oxidation of AA at conventional electrodes is found difficult because of interference due to the co-existence of interfering compounds such as DA and UA, which also undergo oxidation more or less at the same potential. Fig. 2 shows the typical cyclic voltammograms (CVs) of AA, DA and UA on the bare GCE and $NiCoO_2$/C modified GCE. As shown, the oxidation peak potentials of these three molecules are very close to each other at the bare GCE (Fig. 2A). For AA and UA, the electrochemical reactions are irreversible and the signals show broader oxidation peaks with the peak potentials of 0.06 V (AA) and 0.14 V (UA). For DA, the anodic and cathodic peaks appear at −0.08 V and −0.63 V, respectively. These indicate the sluggish electron transfer kinetics at the GCE. In comparison to the bare GCE, the electrochemical reactivity of these three molecules at the $NiCoO_2$/C modified GCE exhibited a significant enhancement (Fig. 2B), and the oxidation peak currents are five larger than those of the GCE. For AA, it displayed a substantial negative shift of the oxidation peak potential to −0.17 V which is about 0.23 V more negative than that at the GCE. In the case of UA, a sharp oxidation peak at 0.05 V and a small reduction peak at −0.33 V are obtained, suggesting that the reversibility of UA at the $NiCoO_2$/C modified GCE is remarkably improved. The anodic and cathodic peaks of DA appear at 0.00 V and −0.54 V, respectively. These results demonstrate that the electron transfer at the $NiCoO_2$/C modified GCE is much easier, so $NiCoO_2$ NPs can accelerate the electron transfer.

Specially, the oxidation potential of AA has the biggest shifting toward negative direction. Because AA, DA and UA have different sensitivity towards the electronic properties, electrode surface microstructure and surface chemistry, the extent of the peak potential shift is different (Huang et al., 2010), which is the key factor to realize simultaneous determination. The general explanation was attributed to the electrostatic interaction between the electroactive sites and analytes (Zhang et al. 2013a). Negatively charged AA is easier to accumulate on the positively charged Ni^{3+}/Co^{3+} modified electrode than positively charged DA. As a result, the modified electrode could more easily electrocatlysis the oxidation of AA than DA. In addition, AA oxidation is an inner-sphere reaction and the electron transfer kinetics is sensitive to the electrode surface properties (Maleki et al., 2006). Therefore, a large negative shift in the oxidation peak potential of AA was obtained, which is beneficial to selective determination of AA from DA and UA.

The probable AA oxidation process on the surface of the $NiCoO_2$/C modified GCE is as follows:

$$NiCoO_2 + 2OH^- \rightarrow NiOOH + CoOOH + 2e^- \quad (1)$$

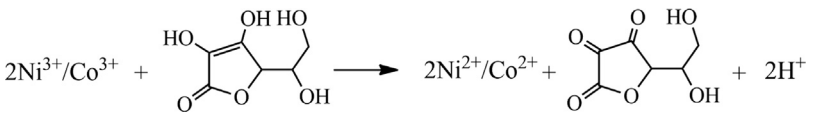

(2)

In alkaline media, $NiCoO_2$ tends to change to NiOOH and CoOOH (Arvinte et al., 2010), as such in reaction (1), which have a high electron and proton conductivity and significant voltammetric response, due to the combined effect of the oxygen donation from Ni and Co oxide/hydroxide (Shen et al., 2010). That can greatly enhance the catalytic activity toward hydroxyl oxidation.

In addition, the hydroxide ion in the alkaline solution tended to neutralize with the decomposed hydrogen ions. The reactions described in the following went forward (Weng et al., 2011):

$$H_2A \rightarrow HA^- + H^+ + e^- \quad (3a)$$

$$HA^- \rightarrow A^{2-} + H^+ + e^- \quad (3b)$$

Thus, the alkaline solution was capable of producing high sensitivity and was therefore adopted in this study. As seen from Fig. S2, in comparison to the pH 7, AA displayed a substantial

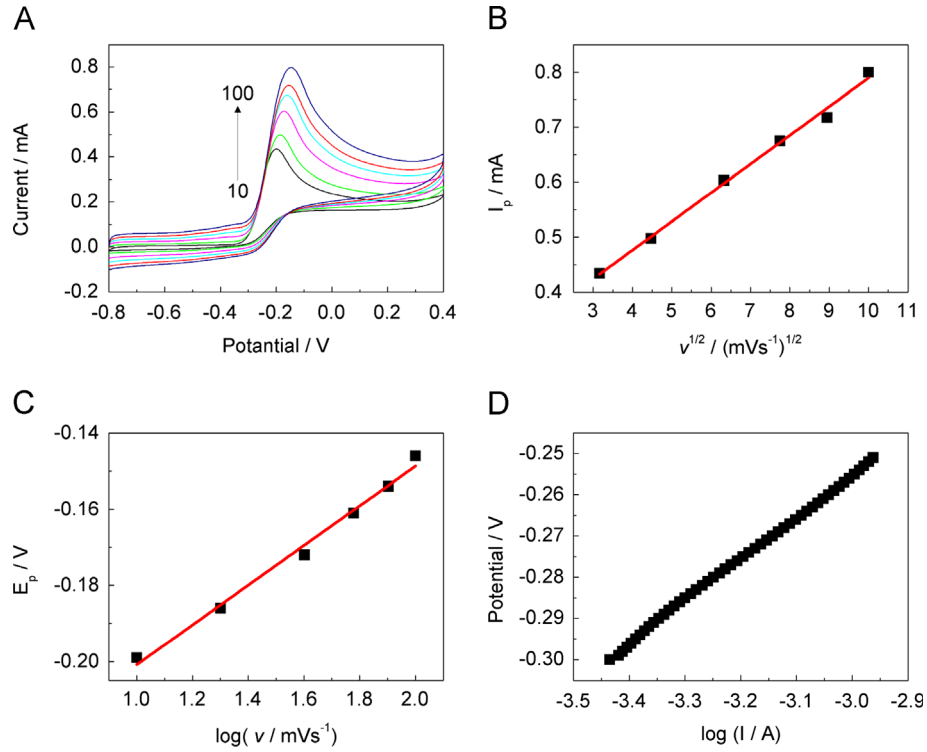

Fig. 3. (A) CVs of the $NiCoO_2$/C modified GCE in 85 mM PBS+5 mM KOH (pH 12.0) with 10 mM AA at various scan rates (10, 20, 40, 60, 80 and 100 mV s^{-1}). (B) The variation of the anodic peak currents vs. $v^{1/2}$. (C) Variation of the anodic peak potential vs. log v. (D) Tafel plot derived from the rising part of voltammogram recorded at a scan rate 10 mV s^{-1}.

negative shift of the oxidation peak potential, and the oxidation peak currents are also increased, that can demonstrate the enhancement of $NiCoO_2$ towards AA oxidation.

Moreover, the current response of the sensor to the concentration of AA was also investigated by cyclic voltammetry, and well-defined current proportional to the AA concentration was observed. Fig. S3 illustrates a series of CVs of $NiCoO_2$/C modified GCE in the presence of different concentrations of AA ranging from 0 to 10 mM in 85 mM PBS+ 5 mM KOH (pH 12.0) solution, and the correlation between the oxidation peak intensity and AA concentration is shown in inset of Fig. S3. As is obvious, the anodic peak current increased constantly with increasing AA concentration, and the plot is linear up to a concentration of 10 mM. The linear regression equation was expressed as follows:

$$I\,(\mathrm{mA}) = 0.007 + 0.041 C_{\mathrm{AA}}\,(\mathrm{mM})\ (R^2 = 0.9994),$$

and the detection limit of 1.0×10^{-5} M was estimated at a S/N of 3.

3.3. Kinetics and mechanism

3.3.1. Effect of scan rate of AA

Fig. 3A shows the CVs of the $NiCoO_2$/C modified GCE in the presence of 5.0 mM AA at various scan rates. As is obvious, the oxidation peak current was observed to increase with increasing scan rate from 10 to 100 mV/s. This result suggests a kinetic limitation in the reaction between redox sites of the $NiCoO_2$/C modified GCE and AA. Meanwhile, the anodic peak current is proportional to the square root of the scan rate (Fig. 3B), indicating a typical behavior for a mass transfer controlled reaction.

In order to get information on the rate-determining step, a plot of E_p vs. log ν (Fig. 3C) revealed a linear behavior with a slope 0.052 V, obeying the following equation, which is valid for a totally irreversible diffusion controlled process (Shamsipur. et al., 2010):

$$E_p = \frac{b}{2}\log \nu + \text{constant} \tag{4}$$

where E_p indicates the oxidation peak potential, and b is Tafel slope (Zare and Chatraei, 2011):

$$b = \frac{2.303RT}{(1-\alpha)nF} \tag{5}$$

where α is the anodic transfer coefficient, n is the number of electrons involved in the rate-determining step and F=96,500 C mol^{-1} is Faraday constant. The slope of the plot in Fig. 3C is 0.0522 V $(\log \nu)^{-1}$, thus, the Tafel slope $b = 2 \times 0.0522$ V, which indicates that one-electron transfer process is the rate determining step by assumption of a transfer coefficient α=0.43 (n=1). Meanwhile, Fig. 3D shows a Tafel plot that was drawn from data of the rising part of current–voltage curve recorded at a scan rate of 10 mV s^{-1}. A slope of 0.1010 V $decade^{-1}$ is obtained, which indicates that a one-electron transfer would be the rate-limiting step, assuming a transfer coefficient of α=0.41. The results are in agreement with those obtained from Fig. 3C.

3.3.2. Chronoamperometric studies

The chronoamperometry was employed for determination of diffusion coefficient of AA and also for obtaining the catalytic rate constant for the reaction between AA and $NiCoO_2$/C modified GCE according to method of Galus. Fig. S4A shows the chronoamperograms obtained for various AA concentrations at $NiCoO_2$/C modified GCE. In chronoamperograms, for an electroactive material, the current response under diffusion control was described by Cottrell equation (Bard and Faulkner, 2001):

$$I = nFD^{1/2}C\pi^{1/2}t^{-1/2} \tag{6}$$

Plots of I vs. $t^{-1/2}$ were constructed (Fig. S4B), with the best fits for different concentrations of AA. The slopes of the resulting straight lines were then plotted vs. AA concentration (Fig. S4D(a)). From the resulting slope and Cottrell equation the value of D was found to be 8.1×10^{-6} cm^2 s^{-1}.

Catalytic rate constant, k, for the reaction between AA and modified electrode was obtained by the method of Galus (1976):

$$\frac{I_C}{I_L} = \pi^{1/2}(kC_b t)^{1/2} \quad (7)$$

where I_C is the catalytic current of AA at $NiCoO_2$/C modified GCE, I_L is the limited current in the absence of AA, C_b is the bulk concentration of AA and t is the time elapsed. Fig. S4C shows the plot of I_C/I_L vs. $t^{1/2}$ obtained from chronoamperograms. From the plotted values of the slopes (Fig. S4D(b)), the equation of k was expressed to be:

$k\ (\mathrm{mM^{-1}\ s^{-1}}) = 1142.5 C_b\ (\mathrm{mM})\ (R^2 = 0.9983)$.

3.4. Selective determination of AA

3.4.1. Amperometric sensing of AA

The amperometric response of the $NiCoO_2$/C modified GCE to successive additions of AA was further evaluated. Fig. 4 shows the amperometric current–time response of AA at −0.20 V. As illustrated, upon addition of an aliquot of AA to the stirred solution containing 85 mM PBS+5 mM KOH (pH 12.0), the oxidation current increased steeply and reached a steady-state current within 3 s. The amperometric signal showed a good linear correlation to AA concentration in the range from 10 μM to 2.63 mM. The linear regression equation was expressed as I_{pa} (mA)=− 0.0086+ 0.0390 C_{AA} (mM) (R^2=0.9929). The current deviates from linearity at higher AA concentrations, most possibly due to the saturation of active sites at the surface of electrode and the passivation of the electrode and/or the formation of 2,3-diketogluconic acid, as this is known to occur in alkaline media (Prieto et al., 1998).

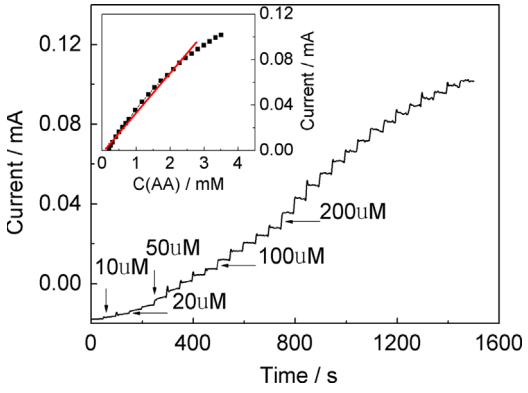

Fig. 4. Amperometric responses of $NiCoO_2$/C modified GCE in 85 mM PBS+5 mM KOH (pH 12.0) at an applied potential of −0.20 V for various concentrations of AA from 0.01 to 3.51 mM.

Table 1 shows the comparison of some response characteristics of the proposed modified electrode with those previously reported. The proposed sensor exhibited high sensitivity with lower overvoltage and broader linear range, which are due to the excellent electrocatalytic activity of $NiCoO_2$ NPs itself towards AA. Furthermore, the current response becomes stable in less than 2 s, which indicates a significantly rapid response of $NiCoO_2$/C towards AA.

3.4.2. Sensor specificity

For selective determination of AA at the $NiCoO_2$/C modified GCE, DPV was carried out in 85 mM PBS+5 mM KOH (pH 12.0) to study the interference of DA and UA. In these measurements, only concentration of the target biomolecule was changed, while concentration of the other biomolecule was kept constant. As shown in Fig. S5, the electrochemical response of AA, DA, or UA increases linearly with the increase of the target biomolecule concentration. It is found that addition of DA and UA into the electrochemical cell does not have significant influence on the peak currents and peak potentials of AA.

The interference experiments were also carried out by successive addition of 0.2 mM AA and 0.20 mM interfering species (glucose, fructose, lactose, sucrose, tryptophan, glycine, $NaNO_2$, UA and DA) in 85 mM PBS+5 mM KOH (pH 12.0). The measured effects of different interferents along with AA at −0.20 V are shown in Fig. 5 For all the interfering species, $NiCoO_2$/C modified GCE did not show any significant fluctuation in the sensor response, and the current responses due to the added interferents ranging were neglected compared to AA. These results indicate that $NiCoO_2$/C modified GCE is highly specific to AA in the presence of various organic and inorganic interfering species normally found in food and biological samples at −0.20 V. These results demonstrate that selective determination of AA on $NiCoO_2$/C modified GCE can be achieved with high sensitivity and selectivity.

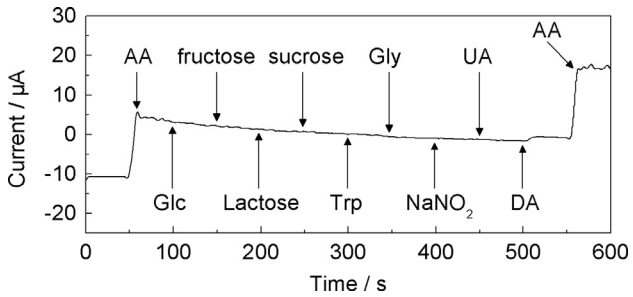

Fig. 5. Interference test of the sensor in 85 mM PBS+5 mM KOH (pH 12.0) at −0.20 V with 0.2 mM AA and other interferents as indicated.

Table 1
Comparison of analytical performance of our proposed $NiCoO_2$/C modified GCE sensor with other published AA sensors.

Electrode material	Applied potential (mV)	Linear range (mM)	Detection limit (μM)	Sensitivity (μA mM^{-1} cm^{-2})	Reference
Au-PANI-GCE	−200	0.01 – 12	8.2	25.69	Zhang et al. (2013b)
OPPy-PdNPs/Au	0	0.001 – 0.52	1	570	Shi et al. (2012)
CoPc-MWNTs/GC	190	0.01 – 2.6	1.0	444.2	Zuo et al. (2012)
CuNPs/c-MWCNT/PANI/Au	400	0.005 – 0.6	1.0	500	Chauhan et al. (2011)
La-MWCNTs modified GCE	80	4×10^{-4} – 0.71	0.14	283.3	Zhang et al. (2012)
Ni foil	200	0.57 – 5.68	–	169	Weng and Hsiao (2011)
Ni–Pt alloys	200	0.57 – 5.68	–	333	Weng et al. (2011)
Graphene/Pt-modified GCE	200	1.5×10^{-4} – 0.034	0.15	1761.5	Sun et al. (2011)
PdNPs-GO/GCE	100	0.02 – 2.28	–	6.148[a]	Wu et al. (2012)
Pd NWs/GCE	0	0.025 – 0.9	0.2	166.5	Wen et al. (2010)
PdNi/C modified GCE	−50	0.01 – 1.80	0.5	760.6	Zhang et al. (2013c)
$NiCoO_2$/C modified GCE	−200	0.02 – 2.41	0.5	549.3	This work

[a] Geometric area is unknown (unit =μA mM^{-1}).

3.5. Reproducibility and stability

The reproducibility of the $NiCoO_2$/C modified GCE for AA determination was investigated with intra- and interassay precision (Fig. S6A). The intraassay precision of the sensor was evaluated by assaying 0.2 mM AA with the same $NiCoO_2$/C modified GCE. The relative standard deviation (RSD) for 10 successive determinations was about 5.7%, demonstrating an excellent detecting reproducibility. Additionally, the interassay precision, or the fabrication reproducibility, was estimated by detecting 0.2 mM AA in duplicate with four sensors prepared in the same manner in dependently. The RSD was 2.0%. Thus, the proposed method had an excellent reproducibility for AA determination.

The storage stability of the designed sensor was also investigated by measuring its sensitivity (S) over three weeks under ambient conditions. For the detection of 0.2 mM AA, there was no significant decrease in current response in the first 7 days, and a 90% response current was still retained after three weeks (Fig. S6B). Therefore, the stability of the proposed electrode was good enough for continual operation.

3.6. AA analytical applications

In order to examine the practical applicability of the $NiCoO_2$/C modified GCE, electrochemical determinations of AA in some real samples (fetal bovine serum (FBS), vitamin C tablets and beverage) were performed. They were firstly diluted in 85 mM PBS+5 mM KOH (pH 12.0), and known amount of standard AA was added into the real sample and recoveries were determined (Table S1). The recoveries are in the range of 97.8–104.8%. The good recoveries for AA indicated the potential usefulness of $NiCoO_2$/C modified electrode for the practical determination of AA in real samples. The AA contents of the FBS were determined to be 0.006 mM and in accordance with the normal value (0.005–0.016 mM after five times diluted). The AA content was determined to be 8.0 mM for vitamin C tablets and 0.023 mM for vitamin C beverage, which are also in accordance with the products facts (8.4 and 0.023 mM after fifty times diluted).

4. Conclusion

A novel sensor has been fabricated based on the carbon-supported $NiCoO_2$ nanoparticles modified GCE. Due to its unique properties, the $NiCoO_2$/C modified GCE exhibited remarkable electrocatalytic effects on the oxidation of AA by increasing their oxidation peak currents and lowering their oxidation peak potentials. The most probable reason for such an increase in sensitivity is the capability of $NiCoO_2$/C modified GCE to accelerate the rate of electron transfer of these compounds, thereby increasing the sensitivity. This was proved by CV and the diffusion coefficient measurements. Furthermore, the modified electrode can clearly distinguish AA in the presence of DA and UA and, thus, is suitable for selective detection of AA without the interference of DA and UA that usually exists in physiological conditions. This proposed method was applied to the determination of AA in pharmaceutical product, beverage, and serum samples with satisfactory results. Thus, $NiCoO_2$/C is a promising candidate for construction of sensitive and selective biosensors. Unfortunately, DA and UA are overlapping, thus simultaneous determination of AA, DA and UA cannot be achieved in this work.

Acknowledgment

We gratefully acknowledge support from the National Natural Scientific Foundation of China (no. 21301137), the New Teachers' Fund for Doctor Stations, Ministry of Education (Grant no. 20126101120012), the Scientific Research Program Funded by Shaanxi Provincial Education Department (Grant nos. 12JK0578 and 12JK0617) and the Scientific Research Foundation of Shaanxi Provincial Key Laboratory (11JS080 and 12JS087).

Appendix A. Supporting information

Supplementary data associated with this article can be found in the online version at http://dx.doi.org/10.1016/j.bios.2013.12.046.

References

Armstrong, R.D., Briggs, G.W.D., Charles, E.A., 1988. J. Appl. Electrochem. 18, 215.
Arvinte, A., Westermann, A.C., Sesay, A.M., Virtanen, V., 2010. Sensors Actuat. B 150, 756.
Bard, A.J., Faulkner, L.R., 2001. Electrochemical Methods: Fundamentals and Applications, 2nd ed. Wiley, New York.
Bertoncello, R., Furlanetto, F., Guerriero, P., Musiani, M., 1999. Electrochim. Acta 44, 4061.
Cao, L., Lin, M., Li, H.L., 2005. J. Electrochem. Soc. 152, A871.
Cattarin, S., Guerriero, P., Musiani, M., 2001. Electrochim. Acta 46, 4229.
Chang, S.-K., Zainal, Z., Tan, K.-B., Yusof, N.A., Yusoff, W.M.D.W., Prabaharan, S.R.S., 2012. Curr. Appl. Phys. 12, 1421.
Chauhan, N., Narang, J., Rawal, R., Pundir, C.S., 2011. Synth. Met. 161, 2427.
Galus, Z., 1976. Fundamentals of Electrochemical Analysis. Ellis Horwood, New York.
Gennero de Chialvo, M.R., Chialvo, A.C., 1993. Electrochim. Acta 38, 2247.
Hossu, A.M., Magearu, V., 2004. Roumanian Biotechnol. Lett. 9, 1497.
Huang, S.H., Liao, H.H., Chen, D.H., 2010. Biosens. Bioelectron. 25, 2351.
King, W.J., Tseung, A.C.C., 1974. Electrochim. Acta 19, 485.
Kumar, S.A., Lo, P.H., Chen, S.M., 2008. Biosens. Bioelectron. 24, 518.
Lin, C., Ritter, J.A., Popov, B.N., 1998. J. Electrochem. Sci. 145, 4097.
Liu, Q., Zhu, X., Huo, Z., He, X., Liang, Y., Xu, M., 2012. Talanta 97, 557.
Maleki, N., Safavi, A., Tajabadi, F., 2006. Analyt. Chem. 78, 3820.
Nam, K.W., Kim, K.B., 2002. J. Electrochem. Soc. 149, A346.
Prieto, F., Coles, B.A., Compton, R.G., 1998. J. Phys. Chem. B 102, 7442.
Rafiee, B., Fakhari, A.R., 2013. Biosens. Bioelectron. 46, 130.
Ragupathy, D., Gopalan, A.I., Lee, K.P., 2010. Sensors Actuat. B 143, 696.
Rashkova, V., Kitova, S., Konstantinov, I., Vitanov, T., 2002. Electrochim. Acta 47, 1555.
Serebrennikova, I., Birss, V.I., 1997. J. Electrochem. Soc. 144, 566.
Shamsipur., M., Najafi, M., Hosseini, M.R.M., 2010. Bioelectrochemistry 77, 120.
Shen, S.Y., Zhao, T.S., Xu, J.B., Li, Y.S., 2010. J. Power Sources 195, 1001.
Shi, W., Liu, C., Song, Y., Lin, N., Zhou, S., Cai, X., 2012. Biosens. Bioelectron. 38, 100.
Srinivasan, V., Weidner, J.W., 2000. J. Electrochem. Soc. 147, 880.
Sun, C.-L., Lee, H.-H., Yang, J.-M., Wu, C.-C., 2011. Biosens. Bioelectron. 26, 3450.
Unates, M.E., Folquer, M.E., Vilche, J.R., Arvia, A.J., 1992. J. Electrochem. Soc. 139, 2697.
Wen, D., Guo, S.J., Dong, S.J., Wang, E.K., 2010. Biosens. Bioelectron. 26, 1056.
Weng, Y.-C., Hsiao, Y.-L., 2011. J. Electroanalyt. Chem. 651, 160.
Weng, Y.-C., Lee, Y.-G., Hsiao, Y.-L., Lin, C.-Y., 2011. Electrochim. Acta 56, 9937.
Wu, G., Li, N., Zhou, D.-R., Mitsuo, K., Xu, B.-Q., 2004. J. Solid State Chem. 177, 3682.
Wu, G.-H., Wu, Y.-F., Liu, X.-W., Rong, M.-C., Chen, X.-M., Chen, X., 2012. Analyt. Chim. Acta 745, 33.
Yoon, Y.I., Ko, J.M., 2008. J. Electrochem. Sci. 3, 1340.
Yuan, A.B., Xu, N.X., 2001. J. Appl. Electrochem. 31, 245.
Zare, H.R., Chatraei, F., 2011. Sensors Actuat. B 160, 1450.
Zhang, B., Huang, D., Xu, X., Alemu, G., Zhang, Y., Zhan, F., Shen, Yan., Wang, M., 2013a. Electrochim. Acta 91, 261.
Zhang, H., Huang, F., Xu, S., Xia, Y., Huang, W., Li, Z., 2013b. Electrochem. Commun. 30, 46.
Zhang, W., Yuan, R., Chai, Y.Q., Zhang, Y., Chen, S.H., 2012. Sensors Actuat. B 166–167, 601.
Zhang, X., Cao, Y., Yu, S., Yang, F., Xi, P., 2013c. Biosens. Bioelectron. 44, 183.
Zuo, X., Zhang, H., Li, N., 2012. Sensors Actuat. B 161, 1074.